Anal Bioanal Chem
DOI 10.1007/s00216-017-0485-5

RESEARCH PAPER

Biosensor of alkaline phosphatase based on non-fluorescent FRET of Eu^{3+}-doped oxide nanoparticles and phosphorylated peptide labeled with cyanine dye

Fan Shi Li[1,2] · Ya Ling Zhang[2] · Xia Bing Li[2] · Bao Lin Li[2] · Yi Feng Liu[1]

Received: 2 February 2017 / Revised: 15 April 2017 / Accepted: 22 June 2017

Abstract Dephosphorylation of biomolecules under the catalysis of alkaline phosphatase (ALP) is a critical physiological process. Abnormal levels of ALP activity have been associated with a number of diseases; thus, a simple and sensitive assay of ALP activity is highly demanded. Herein, to simulate biological conditions, we labeled a hydrosoluble phosphorylated heptapeptide Gly-Pro-Gly-Asn-p-Tyr-Gly-Ala (pGA) with aminated heptamethine cyanine dye (Cy) to give a low fluorescent labeled peptide Cy-pGA. The synthesized Cy-pGA and Eu^{3+}-doped oxide $Y_{0.6}Eu_{0.4}VO_4$ nanoparticles (NPs) were employed respectively as acceptor and donor to in situ form a non-fluorescent Fluorescence Resonance Energy Transfer (FRET) Cy-pGA-NP system, with the help of the strong interaction between Eu^{3+} ions in the NPs and phosphate group in Cy-pGA. The breaking of the FRET system of Cy-pGA-NP was triggered by the removal of phosphate group in Cy-pGA catalyzed by ALP and resulting in the release of fluorescent $Y_{0.6}Eu_{0.4}VO_4$ NPs. Thus, the formed Cy-pGA-NP as a sensitive sensor can very well respond to the activity of ALP by measuring the time-resolved fluorescent intensity at near-infrared 617 nm (λ_{ex} = 320 nm, delay time 400 μs). This sensor can not only accurately measure the activity of ALP (1–5 mU/mL) in the designed solutions, but it can also be applied to detect the activity of ALP in biological samples, such as cell lysate and human serum, without the interference of autofluorescent background of biosamples and screen ALP inhibitor by a simple mix-and-measure manner.

Keywords Biosensors · Alkaline phosphatase · Eu^{3+}-doped oxide · Nanoparticles · Phosphorylated peptide · Cyanine dye

Electronic supplementary material The online version of this article (doi:10.1007/s00216-017-0485-5) contains supplementary material, which is available to authorized users.

✉ Bao Lin Li
baolinli@snnu.edu.cn

✉ Yi Feng Liu
abc981@nwu.edu.cn

[1] Chemical Research Institute, School of Chemical Engineering, Northwest University, Xi'an 710069, China

[2] Key Laboratory of the Ministry of Education for Medicinal Resources and Natural Pharmaceutical Chemistry, National Engineering Laboratory for Resource Development of Endangered Crude Drugs in Northwest of China, School of Chemistry & Chemical Engineering, Shaanxi Normal University, Xi'an 710062, China

Introduction

Phosphorylation and dephosphorylation are critical for many physiological processes [1]. A large fraction of substrates, such as proteins, sugars, lipids, and other molecules, are at least temporarily phosphorylated. Phosphorylation is especially important for protein function as this modification activates (or deactivates) many protein kinases, thereby regulating their function. For instance, the activation of epidermal growth factor receptor (EGFR) tyrosine kinase from its phosphorylation is responsible for cell proliferation, survival, adhesion, migration, and differentiation [2]. Dephosphorylation is the removal of phosphate group from phosphorylated biomolecule by hydrolysis under the catalysis of phosphatase. Many diseases are caused by losing the balance of phosphorylation and dephosphorylation [3]. Alkaline phosphatase (ALP) is one of the most common hydrolase enzymes in mammalian tissues, particularly concentrated in bone, liver, kidney, bile duct, and placenta [4]. Abnormal levels of ALP activity associate with a number of diseases [5], such as osteoporosis, hepatitis, bone

Published online: 24 July 2017

tumor and prostatic cancer, etc. [6]. Therefore, ALP has been used as an important tool in medical diagnosis, molecular biology laboratories, as well as in the dairy industry as an indicator of successful pasteurization [7]. Currently, various methods for the detection of ALP activity have been developed, such as electrochemistry [8], spectrophotometry [9], chemiluminescence [10], surface Raman scattering [11], colorimetric [12], and fluorescence assays [13–16]. Although those reported methods have their own advantages in the detection the activity of ALP, there are still some limitations such as complicated sensing mechanisms, short fluorescence lifetime, short emission wavelength, and autofluorescence interference of biosamples. Thus, the development of convenient and sensitive sensor for the detection of ALP activity is still highly demanded.

In the last two decades, lanthanide (Ln) materials have been extensively used in various fields, such as photoelectric device [17] and biomedical applications including biodetection [18], bioimaging [19], disease theranostics [20], etc. This is because of the excellent chemical and optical properties of lanthanide materials, including long fluorescence lifetime in the millisecond range, narrow emission spectra, large Stokes shift, low toxicity, as well as high resistance to blinking, photochemical degradation, and photobleaching [21]. Among them, Ln-doped inorganic nanoparticles (NPs) are a prominent class of nanocrystals with multicolor emission. Due to the unique $4f^n$ inner shell configurations of Ln^{3+} ions, Ln-doped NPs, rich in magnetic and optical properties, can perform ultrasensitive bioassays in vitro and in vivo [22]. Because of the outstanding features of Ln-doped NPs, we are committed to developing a novel turn-on Ln-doped NP-based fluorescent nano-sensor for the detection of ALP activity and the screening of ALP inhibitors.

Experimental section

Materials and apparatus

All reagents used in this experiment were analytical grade and used directly as obtained commercially unless otherwise stated. HEPES, dithiothreitol (DTT), L-phenylalanine (L-Phe), $Y(NO_3)_3{\cdot}6H_2O$, $Eu(NO_3)_3{\cdot}6H_2O$, $Na_3VO_4{\cdot}12H_2O$, Et_3N, and 6-aminohexanoic acid were obtained from Sigma-Aldrich. Alkaline phosphatases from bovine intestinal mucosa (4500 U/mg) were bought from Shanghai Yuanye Bio-Technology Co., Ltd. Heptapeptide Gly-Pro-Gly-Asn-Tyr-Gly-Ala (GA) and phosphorylated heptapeptide Gly-Pro-Gly-Asn-p-Tyr-Gly-Ala (pGA) were purchased from GL Biochem (Shanghai) Ltd., China. Dulbecco's modified Eagle's medium (DMEM) and fetal bovine serum (FBS) were purchased from Gibco. One-step animal cell active protein extraction kit was bought from Sangon Biotech (Shanghai) Co., Ltd. BCA protein assay kit was purchased from Beijing Biodragon Immunotechnologies Co., Ltd. Human cervical carcinoma Hela cells were kindly donated by Chiatai Tianqing Pharmaceutical Group Co., Ltd.

^{1}HNMR and ^{13}CNMR spectra were recorded on either a Bruker AV 400 or 600 NMR spectrometer. The high resolution mass spectra (HRMS) were measured in ESI negative mode using Bruker maxis UHR-TOF mass spectrometer. Absorption and emission spectra were measured in the 96-well quartz plate (Hellma GmbH & Co., Germany) with Multimode Plate Reader (Enspire, PerkinElmer Co.). The hydrodynamic radius of nanoparticles was measured by using a Malven Autosizer 4700 dynamic light scattering (DLS) spectrometer with scattering angle of 90°.

Preparation of colloidal solution of $Y_{0.6}Eu_{0.4}VO_4$ NPs

The $Y_{0.6}Eu_{0.4}VO_4$ NPs were prepared by slightly modified previous method [23, 24]. In brief, a solution of $Eu(NO_3)_3$ (16 mL, 0.1 M) and $Y(NO_3)_3$ (24 mL, 0.1 M) was added with violent stirring to aqueous solution of Na_3VO_4 freshly in water (40 mL, 0.1 M, pH 12.8) using a peristaltic pump. The addition was stopped when the pH reached to the value of 9.1 (total addition of 30 mL). Then, the mixture is separated by centrifuging (11,240×*g*, 40 min). The obtained precipitate was dispersed in water and sequentially centrifuged (11,240×*g*, 20 min) to obtain $Y_{0.6}Eu_{0.4}VO_4$ NPs as a white powder. The obtained white powder of $Y_{0.6}Eu_{0.4}VO_4$ NPs was re-dispersed in HEPES buffer (10 mM, pH 7.5) under ultrasonic wave for 30 min and then the mixture was stood overnight at 4 °C. The supernatant as a colloidal solution of $Y_{0.6}Eu_{0.4}VO_4$ NPs was collected. The concentration of the NPs is directly indicated by using the concentration of vanadate (VO_4^{3-}) ions (calculated from the absorption intensity at 280 nm from the standard curve shown in Electronic Supplementary Material (ESM), Fig. S1) [23].

Synthesis of activated heptamethine cyanine dye (Cy-NHS)

Preparation of aminated heptamethine cyanine dye (Cy-COOH)

Herein, IR-783 was used as a starting material, and it was prepared according to the reported methods [25].

IR-783 (221.8 mg, 0.305 mmol), Et_3N (365 mg, 3.6 mmol), and 6-aminohexanoic acid (320.4 mg, 2.44 mmol) were dissolved in methanol (50 mL) and the solution was refluxed for 12 h. The solution color changed from green to deep blue. The solvent was removed under vacuum, and the residue was purified by using silica gel column chromatography (MeOH/DCM = 3/1). Cy-COOH was obtained as a deep blue

solid in 77% yield (194.2 mg). HRMS (ESI) ($C_{44}H_{58}N_3O_8S_2Na$) *m/z*: found for $[M]^-$ 820.3646 (calcd 820.3671), $[M]^{2-}$409.6797 (calcd 409.6799). ^{1}H NMR (600 MHz, DMSO-d_6) δ (ppm): 7.48 (d, *J* = 13.0 Hz, 2H), 7.40 (d, *J* = 7.4 Hz, 2H), 7.26 (t, *J* = 7.8 Hz, 2H), 7.07 (d, *J* = 7.8 Hz, 2H), 7.00 (t, *J* = 7.4 Hz, 2H), 5.71 (d, *J* = 13.0 Hz, 2H), 3.87 (t, *J* = 7.2 Hz, 4H), 3.66 (t, *J* = 7.0 Hz, 4H), 2.64 (t, *J* = 7.2 Hz, 2H), 2.02 (t, *J* = 7.4 Hz, 2H), 1.74–1.65 (m, 20H), 1.57 (s, 12H).

Preparation of Cy-NHS

Cy-COOH (36.0 mg, 0.044 mmol) and 1-ethyl-3-(3-dimethylaminopropyl)carbodiimide hydrochloride (EDCI) (20 mg, 0.1 mmol) were dissolved in 1 mL of dry dimethylformamide (DMF) and it was stirred for 15 min, followed by the addition of 1 mL dry DMF solution containing *N*-hydroxysuccinimide (NHS) (5.1 mg, 0.044 mmol) to the above mixture. The obtained mixture was stirred in darkness for 24 h at room temperature under an argon atmosphere. Then, the reaction solution was transferred to a 5-mL volumetric flask and added dry DMF until the total volume reached to 5 mL. This stock solution containing Cy-NHS was directly used to label the peptide without purification.

Labeling of heptapeptide pGA and GA with heptamethine cyanine dye

Synthesis of labeled pGA with heptamethine cyanine dye (Cy-pGA)

pGA (9.6 mg, 0.0135 mmol) and Et_3N (36.5 mg, 0.360 mmol) were dissolved into 1 mL dry DMF, and it was stirred for 15 min. Then, 2 mL of the stock solution of Cy-NHS was added to the reaction system. The obtained mixture was stirred in darkness for 24 h at room temperature under an argon atmosphere. Finally, DMF was evaporated under the vacuum at 70 °C, and the residue was purified by C18 column chromatography (MeOH/H_2O = 1/1) to give the pure Cy-pGA (5.3 mg, 0.0035 mmol, 26% yield). HRMS (ESI) ($C_{71}H_{95}N_{11}O_{20}PS_2$) *m/z*: found for $[M]^{2-}$757.7917 (calcd 757.7933) (see ESM, Fig. S2). The obtained Cy-pGA was dissolved in HEPES buffer (10 mM, pH 7.5) for using as a stock solution at the concentration of 40.0 μM.

Synthesis of labeled GA with heptamethine cyanine dye (Cy-GA)

Following the synthetic method of Cy-pGA, instead of pGA, GA (5.2 mg, 0.0082 mmol) was used in the reaction to give pure Cy-GA (5.1 mg, 0.0035 mmol, 43% yield). HRMS (ESI) ($C_{71}H_{94}N_{11}O_{17}S_2$) *m/z*: found for $[M]^{2-}$717.8094 (calcd 717.8102) (see ESM, Fig. S3). The obtained Cy-GA was dissolved in HEPES buffer which is used as a stock solution.

Time-resolved fluorescence detection of ALP activity by mix-and-measure

ALP stock solution (0~100 μL; 80 mU/mL) and Cy-pGA stock solution (20 μL; 40.0 μM) were added to 100~0 μL of buffer A (10 mM HEPES, 2 mM $MgCl_2$, 2 mM DTT, 0.1% BRIJ-35, 0.1 mM EGTA, pH 7.5) in 96-well quartz plate. After keeping the reaction at 37 °C for 30 min, 100 μL of NP stock solution (0.2 mM) was added to the mixture, and then it was shaken for 1 min. The total volume was controlled in 200 μL. The final concentrations of Cy-pGA and NPs were in 4 μM and 0.1 mM, respectively. And the final concentrations of ALP were from 0 to 40 mU/mL for optimizing the detection range of ALP. Time-resolved fluorescence (TRF) intensity of the system was directly measured at 617 nm (λ_{ex} = 320 nm, delay time 400 μs) by using a Multimode Plate Reader without any further treatment. A regression equation with R^2 = 0.9880, F'/F_0' = 1.01 [ALP] + 0.13, was obtained in the ALP concentration from 1 to 5 mU/mL. Herein, F' and F_0' indicate the fluorescent intensity in the presence or in the absence of ALP.

Under the optimized conditions, the experiment of the inhibition of ALP activity was carried out by mixing a series amount of L-Phe with 7.5 μL of ALP stock solution in buffer A for 20 min at 37 °C, followed by the addition of Cy-pGA stock solution (20 μL) to the above mixture. The obtained mixture was incubated at 37 °C for 30 min. Then, 100 μL of $Y_{0.6}Eu_{0.4}VO_4$ NPs stock solution was added and followed by shaking the mixture for 1 min. In these test solutions, the total volume was 200 μL and the final concentrations of ALP, Cy-pGA, and NPs were in 3 mU/mL, 4 μM, and 0.1 mM, respectively. The final concentrations of L-Phe were controlled from 0 to 87.2 mM. TRF intensity of the mixture was determined at 617 nm (λ_{ex} = 320 nm, delay time 400 μs) on a Multimode Plate Reader. Stronger TRF intensity indicated higher ALP activity. The inhibition ratio (*x*) of L-Phe on ALP was calculated with the following equation:

$$x = 1 - \frac{F_x - F_{01}}{F_1 - F_{01}}$$

F_{01} is the TRF intensity of the mixture of NPs (0.1 mM) and Cy-pGA (4 μM) at 617 nm in buffer A. F_1 is the TRF intensity of the mixture of NPs (0.1 mM), Cy-pGA (4 μM), and ALP (3 mU/mL) at 617 nm in buffer A. F_x is the TRF intensity of the mixture of NPs (0.1 mM), Cy-pGA (4 μM), and ALP (3 mU/mL) in the presence of the different concentration of L-Phe at 617 nm in buffer A.

Cell culture and the activity assay of ALP in cell lysate

The presented procedure is based on our previous report [24]. Hela cells were incubated in DMEM supplemented with 10% (*v*/*v*) FBS, 100 U/mL penicillin, 100 μg/mL streptomycin, and 1% L-glutamate in a humidified incubator containing 5% CO_2 at 37 °C. When the cell confluence was up to 90%, the cultured cells were harvested and lysed with the one-step animal cell active protein extraction kit. In brief, the culture medium was removed, and the cells were washed three times with PBS and then lysed with the lysis buffer on ice for 30 min. The supernatant as a stock solution was collected by centrifugation at 1000×*g* for 10 min and was stored at −80 °C before use [26]. The protein concentration in the stock solution was determined by using a BCA protein assay kit.

The activity assay of ALP in Hela cell lysate was performed by using completely the same method as the detection of ALP activity in above designed solutions, except that ALP stock solution was replaced with a certain volume of the stock solution of Hela cell lysate, and the final protein concentrations of Hela cell lysate were controlled from 0 to 22.1 μg/mL.

Meanwhile, the inhibition of the activity of ALP in Hela cell lysate was performed according to the method discribed in above designed solutions, except that ALP was replaced with Hela cell lysate in the final protein concentration of 0.5 μg/mL, and the final concentrations of L-Phe were from 0 to 120.9 mM. The inhibition ratio of L-Phe on ALP in Hela cell lysate was calculated by using similar equation as aforementioned.

The activity assay of ALP in human serum

Human blood samples were collected from volunteer from the hospital affiliated with Shaanxi Normal University, Xi'an, China. The collected blood samples were centrifuged at 10,000 rpm for 10 min at room temperature. The blood supernatant was stored in a refrigerator at −4 °C and was utilized as a stock solution of serum sample for further experiments.

For the activity detection of ALP in human serum samples, under optimized experimental conditions, 20 μL of 20-fold diluted human serum samples with buffer A, 20 μL of Cy-pGA stock solution, and 60 μL of buffer A were added in 96-well quartz plate. After keeping the reaction at 37 °C for 30 min, 100 μL of the NP stock solution (0.2 mM) was added to the mixture, and then the obtained mixture was shaken for 1 min. TRF intensity of the mixture was directly measured at 617 nm (λ_{ex} = 320 nm, delay time 400 μs) by using a Multimode Plate Reader. The determination of each sample was repeated three times, and each determination set three parallel wells. The concentration of ALP in the serum samples was calculated by the aid of the regression equation obtained from above experiment.

To verify the reliability of the developed ALP assay, medical standard colorimetric analysis with *p*-nitrophenyl phosphate disodium salt (pNPP) [27] was also used to the activity detection of ALP in human serum samples.

Results and discussion

Design, synthesis, and sensing mechanism

Considering the excellent features of Ln-doped NPs, we chose Eu^{3+}-doped oxide NP $Y_{0.6}Eu_{0.4}VO_4$ as a fluorescent donor to design a new non-fluorescent Fluorescence Resonance Energy Transfer (FRET) system for the detection of ALP activity. In the FRET system, a low fluorescent phosphorylated heptapeptide labeled with aminated heptamethine cyanine dye, Cy-pGA, was used as a dark quencher. The mechanism is illustrated in Fig. 1. Previous literatures have demonstrated that Eu^{3+} possesses high binding capacity to phosphate group [28]; thus, a non-fluorescent FRET system, Cy-pGA-NP, should be able to form by capturing Cy-pGA on NP surface with the help of strong interaction between phosphate group in Cy-pGA and Eu^{3+}-doped oxide $Y_{0.6}Eu_{0.4}VO_4$ NP. The breaking of the FRET system was triggered by the removal of phosphate group in Cy-pGA under the catalysis of ALP, resulting in the release of fluorescent $Y_{0.6}Eu_{0.4}VO_4$ NP, while Cy-pGA will be transformed to Cy-GA. Therefore, this non-fluorescent FRET system should be able to respond well to the activity of ALP.

Eu^{3+}-doped NP $Y_{0.6}Eu_{0.4}VO_4$ as a fluorescent donor was prepared according to slightly modified previous method [23, 24]. After re-dispersing the obtained $Y_{0.6}Eu_{0.4}VO_4$ white powder to HEPES buffer under ultrasonic wave 30 min and standing overnight, the supernatant as a colloidal solution of the NPs was collected. The obtained colloidal solution was still stable as homogeneous even after standing for 6 months at 4 °C. The average diameter of the obtained NPs in colloidal solution was measured to be 68 nm by DLS techniques (Fig. ESM, S4a). When the colloidal solution was radiated with 320 nm UV light, the characteristic emission peaks of Eu^{3+} were exhibited at 596 ($^5D_0 \rightarrow {}^7F_1$), 617 ($^5D_0 \rightarrow {}^7F_2$), 652 ($^5D_0 \rightarrow {}^7F_3$), and 700 ($^5D_0 \rightarrow {}^7F_4$) nm (ESM, Fig. S5). These fluorescent emissions owe to that the absorption of UV photons by the VO_4^{3-} group inside the host matrix is followed by nonradiative transfer to the Eu^{3+}, and the latter come back to the ground state through a radiative transition [29]. In all emission peaks, the peak at 617 nm appeared maximal emission intensity; thus, 617 nm was selected for fluorescent detection in this work. Meanwhile, because of long fluorescence lifetime of Ln materials, time-resolved fluorescence (TRF) mode of delay 400 μs was used in the present work to avoid the interference of autofluorescence background of biosamples.

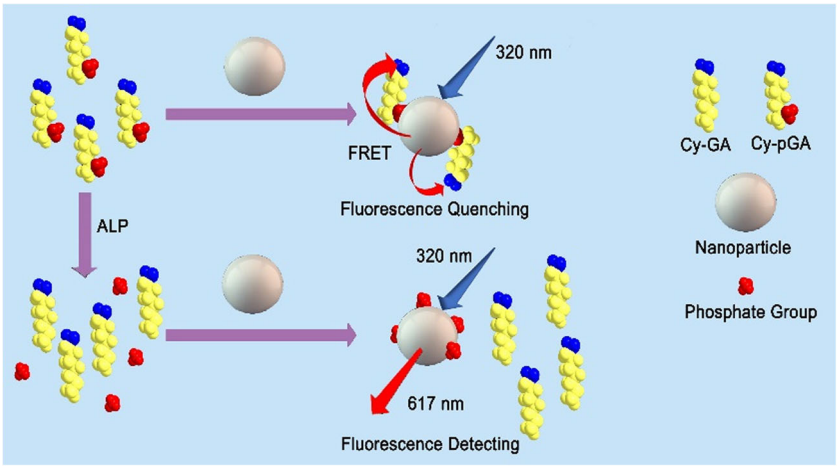

Fig. 1 Design strategy of $Y_{0.6}Eu_{0.4}VO_4$ NPs based on FRET assay for the detection of ALP activity

Previous experiment has demonstrated the aminated cyanine dye (Cy) is a good dark quencher [30]. In non-fluorescent FRET system, the absorption spectrum of dark quencher as an acceptor should overlap with the emission spectrum of donor. Meanwhile, the dark quencher should possess high extinction coefficient. Several amino-heptamethine dyes had been prepared through the nucleophilic substitution of Cl in IR-786 [31], and an obvious change in the wavelength of the absorption maximum from 774 nm of IR-786 to about 626 nm of its aminocyanine dyes was found. In our designed FRET system, Cy-pGA will be used as an acceptor. We would like to synthesize an aminated hydrosoluble analogue of IR-786 to label peptide. Firstly, hydrosoluble heptamethine IR-783 was synthesized according to reported method [25]. Then, the amination of IR-783 was performed with 6-aminohexanoic acid by nucleophilic substitution to give an amino-heptamethine dye (Cy-COOH) in 77% yield (see Scheme 1). The reaction of obtained Cy-COOH and *N*-hydroxysuccinimide in the presence of EDCI gave an activated NHS ester of heptamethine cyanine dye Cy-NHS. The resultant was directly used to label peptide without purification.

To simulate biological condition, a hydrosoluble phosphorylated heptapeptide pGA was selected as the specific substrate of ALP, and it was labeled successfully with heptamethine cyanine dye by the reaction of pGA and Cy-NHS in the presence of Et_3N (see Scheme 1). The labeled peptide Cy-pGA was purified by C18 column chromatography, and its structure was identified by high resolution mass spectrum. Meanwhile, the same sequence unphosphorylated peptide GA was also labeled by Cy with the same method to give a Cy-GA as control compound. The absorption and emission spectra of obtained Cy-pGA and Cy-GA were tested in HEPES buffer (10 mM, pH 7.5). Cy-pGA and Cy-GA showed the same maximum absorption at 620 nm (see ESM, Fig. S6a) and higher molar extinction coefficients (Cy-pGA: $\varepsilon = 3.2 \times 10^4\ M^{-1}\ cm^{-1}$, Cy-GA: $\varepsilon = 3.1 \times 10^4\ M^{-1}\ cm^{-1}$). In addition, they also exhibited very low fluorescent intensity at 740 nm (λ_{ex} = 620 nm) (see ESM, Fig. S6b). As shown in Fig. 2a and ESM, Fig. S6a, the absorption spectra of Cy-pGA and Cy-GA overlapped perfectly with the emission spectrum of $Y_{0.6}Eu_{0.4}VO_4$ NPs. These suggested Cy-pGA may have high potential to be applied as a dark quencher in the designed non-fluorescent FRET system.

The formation of non-fluorescent FRET system

With synthesized $Y_{0.6}Eu_{0.4}VO_4$ NPs and Cy-pGA in hand, we tested whether fluorescent $Y_{0.6}Eu_{0.4}VO_4$ NPs can form a non-fluorescent FRET system with low fluorescent Cy-pGA. We found that the fluorescent intensity of colloidal solution of the NPs obviously reduced immediately at 596, 617, 652, and 700 nm when adding Cy-pGA to the solution of 0.02 mM $Y_{0.6}Eu_{0.4}VO_4$ NPs in buffer A. As shown in Fig. 2b, with the increase of the concentration of Cy-pGA from 0 to 152 μM, the fluorescent intensity of the NP solution at 617 nm (delay 400 μs, λ_{ex} = 320 nm) declined gradually. When the concentration of Cy-pGA was 119 μM, the fluorescence of the NPs was reduced to the weakest. To explore the essential reason of the fluorescent change, instead of Cy-pGA, the same amount of unphosphorylated counterpart Cy-GA was added to the NP solution and no change of fluorescence was observed. These results indicated definitely that FRET has occurred between the NPs and Cy-pGA because of the self-assemblage formation of Cy-pGA-NP, resulting from very close proximity of Cy-pGA and NP. It also suggested that the phosphate group in Cy-pGA is very important for pulling Cy-pGA to the surface of NPs through the strong interaction between Eu^{3+} ions and phosphate groups. Further, we mixed the NPs (0.02 mM) with Cy-pGA or Cy-GA in the same amount, respectively. After 30 min, two mixtures were centrifuged, and the absorptions of their supernatants were measured at 620 nm. The absorption of the supernatant of Cy-pGA with the NPs showed slight reduction comparing with that of the Cy-pGA solution (ESM, Fig. S7a). However, the absorption of the supernatant of Cy-GA with the NPs was the

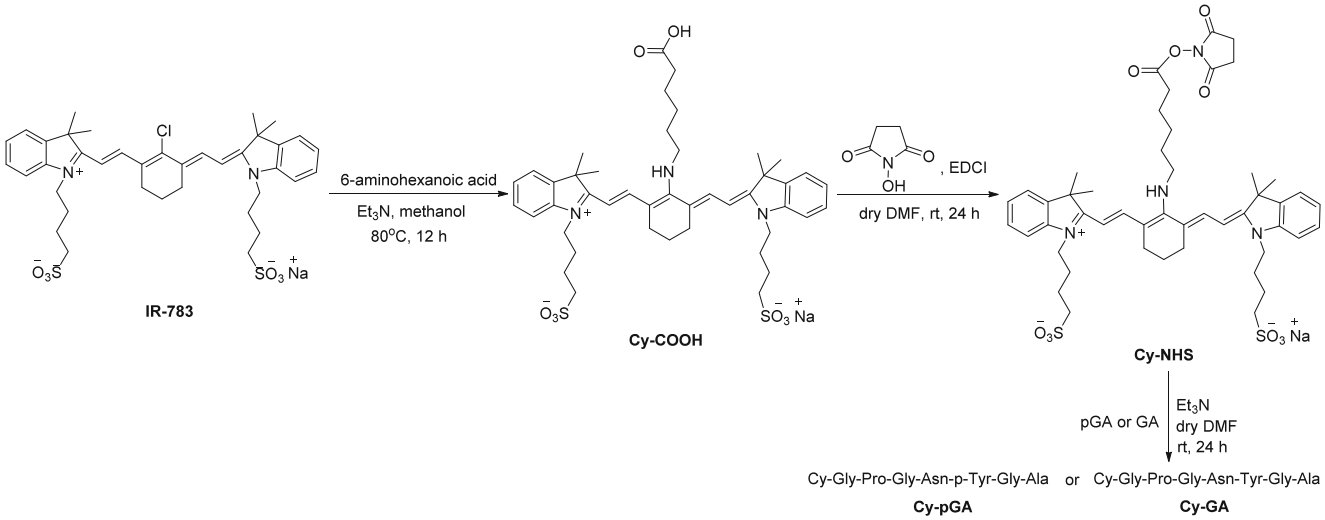

Scheme 1 Synthesis of Cy-pGA and Cy-GA

same as that of the Cy-GA solution (see ESM, Fig. S7b). The absorption at 620 nm attributes to the existence of Cy moiety in Cy-pGA or Cy-GA. Comparing to the absorption of the supernatant from the mixture of Cy-GA and the NPs, the reduced absorption of the supernatant from the mixture of Cy-pGA with the NPs also indicated affirmatively that Cy-pGA was captured to the surface of Eu^{3+}-doped NPs under the help of phosphate group. This led to Cy-pGA precipitating together with the NPs from the supernatant under centrifugal condition. This further demonstrated clearly that the phosphate group in Cy-pGA plays an important role in the formation of designed FRET, although there are carboxyl and sulfonic acid groups in Cy-pGA. Meanwhile, we would like to investigate if the aggregation of NPs could occur when Cy-pGA was added. Thus, the size of the NPs was determined by using DLS techniques. The result indicated the diameter of the NPs was 71 nm (ESM, Fig. S4b), and the aggregation of NPs was not observed.

TRF assay of ALP

Using the developed FRET system, we pursued a highly sensitive biosensor for the assay of ALP. Firstly, the condition of fluorescent quenching was optimized. The same amount of Cy-pGA was added to the solution of the NPs in buffer A to make a series of solutions in different concentrations of the NPs (0.05–0.21 mM) and the same concentrations of Cy-pGA (4 μM). Their fluorescent intensity ratios F/F_0 at 617 nm (F and F_0 indicate the fluorescent intensity after and before introducing Cy-pGA, respectively) were measured (λ_{ex} = 320 nm, delay 400 μs) and exhibited an obvious change with the increasing concentration of NPs (see ESM, Fig. S8). A lower F/F_0 represents a greater difference of the fluorescent intensities between the presence and absence of Cy-pGA. The low F/F_0 could lead to higher detection sensitivity. The result indicated that the concentration of the NPs from 0.08 to 0.16 mM is suitable to build highly sensitive FRET system. Herein, the NP concentration of 0.1 mM along with Cy-pGA concentration of 4 μM was selected for the formation of non-fluorescent FRET system in the experiment of ALP assay.

Under the optimized condition of the formation of non-fluorescent FRET system, the assay of ALP was explored. The response of the FRET system to ALP was observed from the fluorescent recovery of the NPs at 617 nm (λ_{ex} = 320 nm, delay 400 μs) in the presence of ALP. Initially, the mixture of

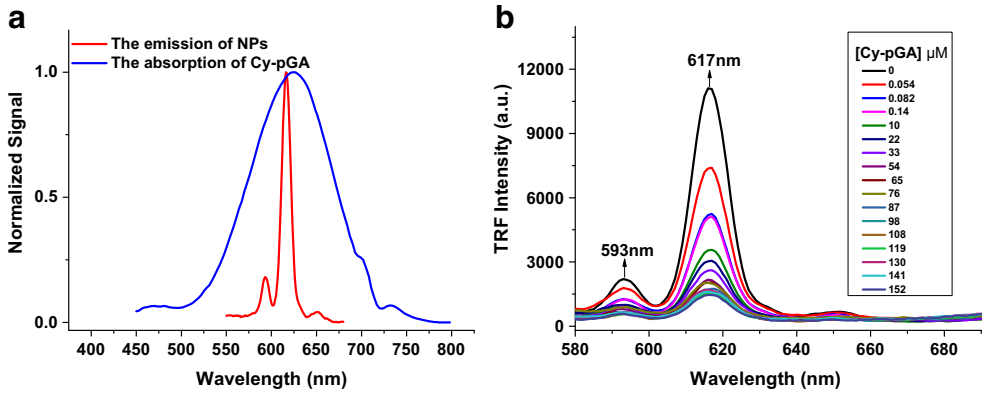

Fig. 2 **a** The emission spectrum of $Y_{0.6}Eu_{0.4}VO_4$ NPs and the absorption spectrum of Cy-pGA in HEPES buffer (10 mM, pH 7.5). **b** The quenching effect of Cy-pGA on the fluorescence of the NPs (the final concentration of the NPs was in 0.02 mM)

ALP with Cy-pGA in buffer A was incubated at 37 °C for 60 min, and then, the NPs were added to the mixture to make the final concentrations of ALP to 10 mU/mL, NPs to 0.1 mM, and Cy-pGA to 4 μM. After vibrating the mixture for 1 min, the fluorescent recovery of the NPs was obviously observed. When the incubation time was reduced to 30 min, the same fluorescent intensity could still be obtained. Thus, the incubation of 30 min at 37 °C was applied to the following experiments. Similarly, the aggregation of the assemblage Cy-pGA-NP did not obviously occur when ALP was added to the solution of the mixture of the NPs and Cy-pGA. This result was deduced from the relevant experiments of DLS (ESM, Fig. S4c). Under this optimized condition, three parallel experiments were carried out to investigate the detection range of ALP. As shown in Fig. 3a, with the increase of the concentration of ALP from 0 to 15 mU/mL, the fluorescent intensity of the system at 617 nm was gradually increased nearly six times comparing to that without ALP. After the concentration of ALP reached 15 mU/mL, the fluorescent intensity and fluorescent intensity ratio F'/F_0' (F' and F_0' indicate the fluorescent intensity in the presence or in the absence of ALP) did not increase anymore (Fig. 3a inset). These facts indicated definitely the Cy-pGA-NP self-assemblage had disintegrated, which led to the breaking of the FRET system and "turn-on" the fluorescence of NPs. This result is caused by the dephosphorylation of Cy-pGA under the catalysis of ALP. Meanwhile, we can see a good linear relationship between the fluorescent ratios F'/F_0' and the ALP concentration from 1 to 5 mU/mL (Fig. 3a inset). The regression equation is $F'/F_0' = 1.01\,[\mathrm{ALP}] + 0.13$ with $R^2 = 0.9880$. The limit of detection (LOD) of ALP in our assay is determined to be 0.37 mU/mL, which is similar to the data from reported methods [15, 16]. This indicated that a good sensor of ALP has been established based on non-fluorescent FRET system formed by the use of Eu^{3+}-doped oxide $Y_{0.6}Eu_{0.4}VO_4$ nanoparticles and the phosphorylated peptide labeled with cyanine dye. The construction of this sensor only needs a very easy mix-and-measure manner.

The activity assay of ALP in cell lysate and human serum

To further demonstrate the feasibility of the sensor to monitor the activity of ALP in real biological samples, the activity detection of ALP in Hela cell lysate and human serum was explored. In these tests, it was found that the major interferences came from the autofluorescent background of biosamples. Initially, we delayed the collection of the fluorescent signals for 1 μs at 617 nm for the mixtures of buffer A, NPs, and ALP or Hela cell lysate or human serum, respectively. The autofluorescent background of each biosample was observed from 400 to 700 nm (see ESM, Fig. S9a). Especially, the mixture containing human serum exhibited stronger autofluorescent background in this range. Because the lifetime of the autofluorescence is obviously shorter than that of NPs, the TRF mode of delaying the collection of the fluorescent signals for 400 μs was used in the detection of ALP in every sample to eliminate the interferences of autofluorescent background. A good result was obtained as shown in ESM, Fig. S9b.

We herein used Hela cell lysate as a biological sample to determine ALP activity by the established method, because Hela human cervical carcinoma cell line is well known to express endogenous ALP [2]. The replacement of ALP to Hela cell lysate and the fluorescent intensities of the mixtures of cell lysate, Cy-pGA (4 μM), and NPs (0.1 mM) in buffer A were enhanced with the increase of the protein concentrations of cell lysate from 0 to 22.1 μg/mL (see Fig. 3b). Monitoring the fluorescent intensity of the mixture at 617 nm (λ_{ex} = 320 nm, delay time 400 μs), the fluorescent intensity ratio F'/F_0' of the mixture showed a linear increasing

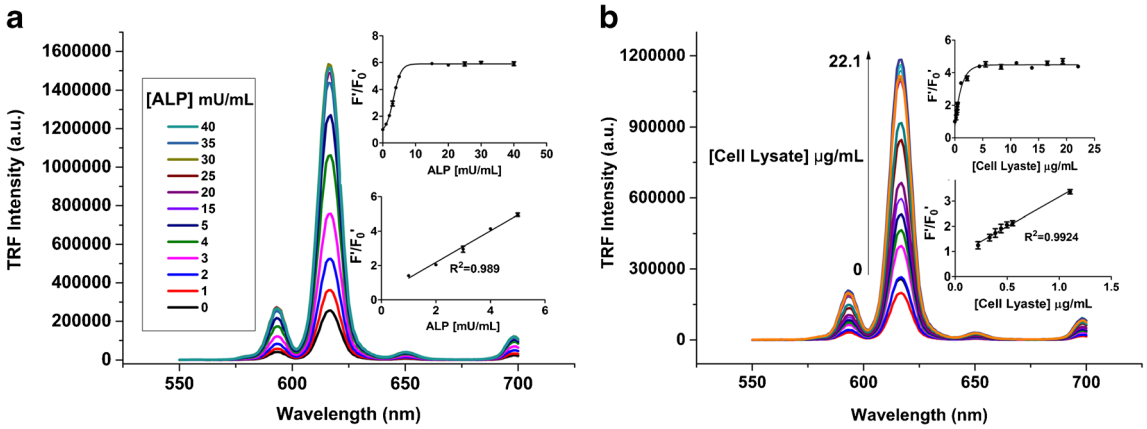

Fig. 3 The change of TRF intensity of the assemblage Cy-pGA-NP (the concentrations of NPs and Cy-pGA in 0.1 mM and 4 μM, respectively) in buffer A with the increase of the concentration of **a** ALP or **b** Hela cell lysate (λ_{ex} = 320 nm, delay 400 μs). (*Inset*: the linear relationship of TRF intensity ratio F'/F_0' to the concentration of ALP or Hela cell lysate, where F' and F_0' stand for the TRF intensity in the presence and absence of ALP or Hela cell lysate)

Table 1 Comparison of results from the colorimetric and the developed determination for the activity of ALP in human serum

Sample	ALP activity (mU/mL)[a]	
	Developed determination[b]	Colorimetric determination[c]
Human serum A	59.47 ± 2.0	64.47 ± 1.4
Human serum B	56.50 ± 1.4	63.31 ± 1.9
Human serum C	65.30 ± 2.0	65.91 ± 2.3
Human serum D	49.51 ± 1.4	46.88 ± 1.7

[a] The determination of each sample was repeated three times, and each determination set three parallel wells

[b] The determination was carried out after diluting human serum samples to 20-fold with buffer A. ALP activity was obtained from 20 times calculated value by the aid of the regression equation $F'/F_0' = 1.01\ [\mathrm{ALP}] + 0.13$

[c] Human serum samples were directly used in the determination

relationship with the increasing of the protein concentrations of the cell lysate from 0.22 to 1.10 μg/mL and it was then reached to a plateau after the protein concentration of cell lysate was up to 5 μg/mL (see Fig. 3b inset). The result indicated the in situ formed Cy-pGA-NP sensor is very well responsive to the activity of ALP in this biological sample and can be used to detect the activity of ALP in biosample through this simple manner.

In order to further evaluate the applicability of the developed sensor in real biosamples, the determination of the activity of ALP in four diluted human serum samples was performed. As shown in Table 1, the activities of ALP in four samples were in the range from 49.51 to 65.50 mU/mL. The SD of detection ranged from 1.4 to 2.0, which were satisfactory for quantitative assays performed in biological samples. Although the linear range of 1–5 mU/mL is not attractive, after diluting human serum samples to 20–30-fold, it is wide enough for health diagnoses since the standard activity of ALP in blood for a healthy male is 55–125 mU/mL (cf. 40–100 mU/mL for a female) [32]. To check the reliability of the developed method, four human serum samples were also determined by medical standard colorimetric analysis with pNPP [27]. In this colorimetric analysis, the hydrolysis of pNPP generated *p*-nitrophenol under the catalysis of ALP. The absorbance of *p*-nitrophenol at 405 nm was related to the activity of ALP. The data of the colorimetric analysis agreed well with that of Cy-pGA-NP system assay. The result indicated the developed sensor is enough for the detection the activity of ALP in real biosamples.

Response of the sensor on ALP inhibitor

ALP has been identified as an important drug target for the potential treatment of some diseases. Selective inhibitors of ALP, thus, may have therapeutic potential [33]. To investigate the application of this sensor in the screening of ALP inhibitor, L-phenylalanine, an ALP inhibitor [34], was used to check the response of the sensor to ALP inhibitor. Under optimized condition, the experiment of the inhibition of ALP activity was carried out by mixing a series amount of L-Phe with ALP in buffer A for 20 min at 37 °C, followed by adding Cy-pGA to above mixture. The obtained mixture was incubated 30 min at 37 °C. Then, $Y_{0.6}Eu_{0.4}VO_4$ NPs was added to the reaction system (the final concentrations of ALP, Cy-pGA, and NPs were in 3 mU/mL, 4 μM, and 0.1 mM, respectively). It was found the TRF intensity of the system was gradually decreased at 617 nm (λ_{ex} = 320 nm, delay time 400 μs) with the increasing concentration of L-Phe. The TRF intensity responded well to the concentration of L-Phe (Fig. 4a). In essence, with the increase of the concentration of L-Phe, the activity of ALP was reduced gradually. Thus, the amount of the formed Cy-pGA-NP was raised due to the slowing down hydrolysis of Cy-pGA in the presence of low active ALP. This led to the system exhibiting lower TRF intensity at 617 nm. Further, the inhibition ratio of ALP activity was calculated as shown in Fig. 4a (inset). And IC_{50} of 22.24 mM for L-Phe was obtained by using the sigmoidal fit.

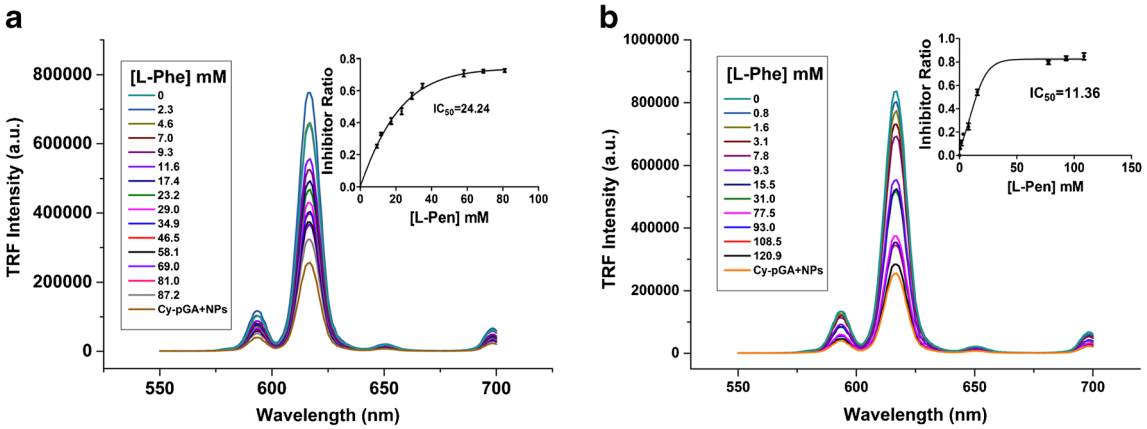

Fig. 4 **a** The activity of ALP was inhibited by different concentration of L-Pen in buffer A. **b** The activity of ALP in Hela cell lysate was inhibited by different concentration of L-Pen in buffer A. The TRF signals at 617 nm were collected by excitation at 320 nm and delay 400 μs

Similar results including IC_{50} of 11.36 mM were also obtained from the replacement of ALP with the Hela cell lysate in the final protein concentration of 0.5 μg/mL (Fig. 4b). These results indicated the sensor can sensitively respond to ALP inhibitor and could be extended to screen ALP inhibitors.

Conclusions

A fluorescent biosensor of alkaline phosphatase was developed based on non-fluorescent FRET formed from Eu^{3+}-doped oxide nanoparticles and the phosphorylated peptide labeled with cyanine dye. In the FRET, fluorescent Eu^{3+}-doped oxide $Y_{0.6}Eu_{0.4}VO_4$ nanoparticles acted as a donor and captured the phosphorylated peptide labeled with aminated heptamethine cyanine dye as a dark quencher on its surface to form a non-fluorescent self-assemblage Cy-pGA-NP, which owe to the strong interaction between Eu^{3+} ions in the NPs and phosphate group in Cy-pGA. When Cy-pGA-NP was irradiated with 320-nm light, the VO_4^{3-} inside the host matrix absorbed and transferred energy to the Eu^{3+}, the latter came back to the ground state with radiating 617 nm near-infrared light. The fact is that the very short distance between Cy-pGA and the NPs caused the aminated Cy in Cy-pGA to absorb and quench this near-infrared light at 617 nm. So, in situ formed Cy-pGA-NP as an ALP sensor can respond to the activity of ALP through measuring the fluorescent intensity at 617 nm, because the breaking of FRET resulted from the hydrolysis of phosphate group in Cy-pGA under the catalysis of ALP. This work provides four significant advancements over existing technologies. That includes (1) based on long fluorescence lifetime feature of Eu in the millisecond range, a time-resolved fluorescence assay with a delay of 400 μs was used to avoid the interference of autofluorescent background of biosamples; (2) the detection of ALP activity in a simple manner by mix-and-measure; (3) the method can be applied in real biological samples such as cell lysate and human serum; and (4) this sensor can be applied in the screening of ALP inhibitor.

Acknowledgements We are grateful to the financial support from the National Natural Science Foundation of China (No. 21272144) and the Fundamental Research Funds for the Central Universities of Shaanxi Normal University (No. X2015YB06).

Compliance with ethical standards

Conflict of interest The authors declare that they have no competing interests.

References

1. Kikuchi I, Takahashi-Kanemitsu A, Sakiyama N, Tang C, Tang PJ, Noda S, et al. Dephosphorylated parafibromin is a transcriptional coactivator of the Wnt/Hedgehog/Notch pathways. Nat Commun. 2016;7:12887.
2. Begley MJ, Yun CH, Gewinner CA, Asara JM, Johnson JL, Coyle AJ, et al. EGF-receptor specificity for phosphotyrosine-primed substrates provides signal integration with Src. Nat Struct Mol Biol. 2015;22:983–90.
3. Sur S, Agrawal DK. Phosphatases and kinases regulating CDC25 activity in the cell cycle: clinical implications of CDC25 overexpression and potential treatment strategies. Mol Cell Biochem. 2016;416:33–46.
4. Fernandez NJ, Kidney BA. Alkaline phosphatase: beyond the liver. Vet Clin Path. 2007;36:223–33.
5. Pike AF, Kramer NI, Blaauboer BJ, Seinen W, Brands R. A novel hypothesis for an alkaline phosphatase 'rescue' mechanism in the hepatic acute phase immune response. Biochim Biophys Acta. 1832;2013:2044–56.
6. Gyurcsanyi RE, Bereczki A, Nagy G, Neuman MR, Lindner E. Amperometric microcells for alkaline phosphatase assay. Analyst. 2002;127:235–40.
7. Albillos SM, Reddy R, Salter R. Evaluation of alkaline phosphatase detection in dairy products using a modified rapid chemiluminescent method and official methods. J Food Prot. 2011;74:1144–54.
8. Miao P, Ning L, Li X, Shu Y, Li G. An electrochemical alkaline phosphatase biosensor fabricated with two DNA probes coupled with lambda exonuclease. Biosens Bioelectron. 2011;27:178–82.
9. Bianchi A, Giachetti E, Vanni P. A continuous spectrophotometric assay for alkaline phosphatase with glycerophosphate as substrate. J Biochem Biophys Methods. 1994;28:35–41.
10. Jiang H, Wang X. Alkaline phosphatase-responsive anodic electrochemiluminescence of CdSe nanoparticles. Anal Chem. 2012;84:6986–93.
11. Ruan C, Wang W, Gu B. Detection of alkaline phosphatase using surface-enhanced Raman spectroscopy. Anal Chem. 2006;78:3379–84.
12. Choi Y, Ho NH, Tung CH. Sensing phosphatase activity by using gold nanoparticles. Angew Chem Int Ed. 2007;46:707–9.
13. Qian ZS, Chai LJ, Huang YY, Tang C, Shen JJ, Chen JR, et al. A real-time fluorescent assay for the detection of alkaline phosphatase activity based on carbon quantum dots. Biosens Bioelectron. 2015;68:675–80.
14. Kang W, Ding Y, Zhou H, Liao Q, Yang X, Yang Y, et al. Monitoring the activity and inhibition of alkaline phosphatase via quenching and restoration of the fluorescence of carbon dots. Microchim Acta. 2015;182:1161–7.
15. Qu F, Pei H, Kong R, Zhu S, Xia L. Novel turn-on fluorescent detection of alkaline phosphatase based on green synthesized carbon dots and MnO2 nanosheets. Talanta. 2017;165:136–42.
16. Zhang W, Gao Y, Li Y, Zhang Q, Hu Z, Zhang Y, et al. Polyphosphoric acid-induced perylene probe self-assembly and label-free fluorescence turn-on detection of alkaline phosphatase. Anal Bioanal Chem. 2017;409:1031–6.
17. Wei W, Zhang Y, Chen R, Goggi J, Ren N, Huang L, et al. Cross relaxation induced pure red upconversion in activator- and sensitizer-rich lanthanide nanoparticles. Chem Mater. 2014;26:5183–6.
18. Zheng W, Huang P, Tu D, Ma E, Zhu H, Chen X. Lanthanide-doped upconversion nano-bioprobes: electronic structures, optical properties, and biodetection. Chem Soc Rev. 2015;44:1379–15.
19. Zeng S, Wang H, Lu W, Yi Z, Rao L, Liu H, et al. Dual-modal upconversion fluorescent/X-ray imaging using ligand-free hexagonal phase $NaLuF_4$:Gd/Yb/Er nanorods for blood vessel visualization. Biomaterials. 2014;35:2934–41.
20. Li W, Wang J, Ren J, Qu X. Near-infrared upconversion controls photocaged cell adhesion. J Am Chem Soc. 2014;136:2248–51.

21. Li H, Wang L. NaYF4:Yb^{3+}/Er^{3+} nanoparticle-based upconversion luminescence resonance energy transfer sensor for mercury(II) quantification. Analyst. 2013;138:1589–95.
22. Wang S, Wang L. Lanthanide-doped nanomaterials for luminescence detection and imaging. TrAC Trends Anal Chem. 2014;62:123–34.
23. Casanova D, Giaume D, Gacoin T, Boilot J-P, Alexandrou A. Single lanthanide-doped oxide nanoparticles as donors in fluorescence resonance energy transfer experiments. J Phys Chem B. 2006;110:19264–70.
24. Li BH, Zhang YL, Li FS, Wang W, Liu J, Liu M, et al. A novel sensor for the detection of alkaline phosphatase activity based on the self-assembly of Eu^{3+}-doped oxide nanoparticles and heptamethine cyanine dye. Sensor Actuat B-Chem. 2016;233:479–85.
25. Wang L, Jin J, Chen X, Fan HH, Li BK, Cheah KW, et al. A cyanine based fluorophore emitting both single photon near-infrared fluorescence and two-photon deep red fluorescence in aqueous solution. Org Biomol Chem. 2012;10:5366–70.
26. Kim TI, Kim H, Choi Y, Kim Y. A fluorescent turn-on probe for the detection of alkaline phosphatase activity in living cells. Chem Commun (Camb). 2011;47:9825–7.
27. Han Z, Huang Z, Lu Y, Hu Y. Automatic analysis of clinical chemistry project. third ed. Shenyang: Liaoning science and technology press; 2005.
28. Liu C, Chang L, Wang H, Bai J, Ren W, Li Z. Upconversion nanophosphor: an efficient phosphopeptides-recognizing matrix and luminescence resonance energy transfer donor for robust detection of protein kinase activity. Anal Chem. 2014;86:6095–102.
29. Huignard A, Gacoin T, Boilot J-P. Synthesis and luminescence properties of colloidal YVO_4:Eu phosphors. Chem Mater. 2000;12:1090–4.
30. Peng X, Xu X, Draney DR, Little GM, Chen J, Volcheck WM. Preparation of nonfluorescent near-IR quencher cyanine dyes for probe labeling. USA **8227621**: LI-COR, Inc.; 2012.
31. Kiyose K, Aizawa S, Sasaki E, Kojima H, Hanaoka K, Terai T, et al. Molecular design strategies for near-infrared ratiometric fluorescent probes based on the unique spectral properties of aminocyanines. Chem. 2009;15:9191–200.
32. Burtist C, Ashwood E. Tietz textbook of clinical chemistry. second ed. Philadelphia: WB Saunders; 1994.
33. al-Rashida M, Iqbal J. Inhibition of alkaline phosphatase: an emerging new drug target. Mini-Rev Med Chem. 2015;15:41–51.
34. Kim SH, Shidoji Y, Hosoya N. Multiple form of L-phenylalanine sensitive alkaline phosphatase in rat fecal extracts. Jap J Exp Med. 1986;56:251–5.